# Role of the Intermediate-conductance Calcium-activated Potassium Channel, KCa3.1, in Cellular Activation and Atherogenesis

## Supporting online material

## Supplemental Results

***Safety profile of KCa3.1 blockers.*** To determine the safety profile of clotrimazole and TRAM-34, we monitored clinical parameters (body wt, heart wt, BP and heart rate), blood chemistry, blood counts and histopathology in apoE$^{+/+}$ mice and in apoE$^{-/-}$ mice treated with the vehicle or with clotrimazole or TRAM-34 during the 12 wk trial (Supplemental Tables 1 and 2). Blood cholesterol levels of apoE$^{-/-}$ mice were dramatically elevated compared to apoE$^{+/+}$ mice (1377 mg/dL versus 70 mg/dL). Clotrimazole and TRAM-34 ameliorated atherosclerosis in apoE$^{-/-}$ mice without reducing the blood cholesterol levels. TRAM-34 did not cause any discernable change in the clinical parameters, blood counts or blood chemistry, when compared to vehicle-treated apoE$^{-/-}$ mice. Unlike KCa3.1$^{-/-}$ mice that develop an increase in mean BP (7 mmHg) and mild left ventricular hypertrophy (1), we did not observe any change in BP or in cardiac size in apoE$^{+/+}$, apoE$^{-/-}$ or C57BL/J mice treated with the therapeutic dose of clotrimazole or TRAM-34. Rats treated with TRAM-34 for six months also did not show any cardiac hypertrophy (data not shown). A body wt reduction of 17% was seen in clotrimazole-treated mice, which was accompanied by a significant increase in the levels of total

protein, globulin, calcium and the anion gap; no other change was noted. One mouse in the vehicle group and in the TRAM-34 group died due to unknown reasons during the treatment.

In parallel toxicological experiments, normal C57BL/6J (apoE$^{+/+}$) mice treated with TRAM-34 for 4 wk did not exhibit any signs of toxicity or show visible abnormalities in the aortas or macroscopic organ damage (Supplemental Table 3).

KCa3.1 expression in the aortas of TRAM-34-treated mice was similar to that in vehicle-treated mice. KCa3.1 was localized to the EC layer of aortas in C57BL6J mice treated with vehicle (Figures 1B, C and I) and this KCa3.1 expression was abolished by EC denudation (Figure 1I and Supplemental Figure 8). Thus, long-term pharmacological blockade of KCa3.1 has no obvious effect on endothelial KCa3.1 expression in aortas (Supplemental Figure 8). Therefore treatment with TRAM-34 has no effect on KCa3.1 expression in ECs in normal mice.

Because of its immunosuppressive effects on T cells and macrophages, KCa3.1 blockers might compromise the immune response to acute infections. C57BL/J mice that received TRAM-34 for 4 wk did not show any histopathological changes in the spleen or thymus (Supplemental Table 3) and patients who were treated with ICA-17043 for 12 wks had no adverse events of infectious diseases, suggesting that chronic dosing with KCa3.1 blockers does not compromise the immune response to infectious agents (2). To further investigate this issue we used the established rat influenza model (3) to examine whether TRAM-34 treatment might delay the clearance of influenza virus. Sprague Dawley rats received TRAM-34 at a dose (20 mg/kg i.p.) that achieves peak plasma

concentrations of 3 μM or vehicle (peanut oil) for one wk before intranasal challenge with rat-adapted influenza virus (2 x $10^5$ pfu) and for 3 wk thereafter (Supplemental Figure 9). As a positive control, another group of rats was administered dexamethasone. Vehicle-treated rats cleared the virus in 4 days, as did TRAM-34-treated rats, while dexamethasone significantly delayed clearance due to its profound and broad immunosuppressive effects.

## Supplemental Materials and Methods

**Reagents** Fluo-4, dihydroethidine (Molecular Probes), 1-EBIO (Tocris Cookson), pimaric acid (Alomone), TRAM-34, TRAM-7, TRAM-3 (synthesized by H.W.) and clotrimazole (Sigma) for in-vitro experiments were dissolved in dimethyl sulfoxide. Glibenclamide was prepared as described previously (4). Charybdotoxin, apamin, and iberiotoxin (Sigma) were dissolved in cell culture medium or PBS with 0.1% BSA. Recombinant mouse MCP-1 and human PDGF-BB were reconstituted according to manufacturer's instructions (R&D Systems). All others were dissolved in distilled water. For in-vivo studies TRAM-34 and clotrimazole was dissolved in peanut oil (Sigma). All concentrations represent the final molar concentrations (mol/L) in the organ chambers or culture dishes. Sudan-III solution was purchased from The Science Company.

**Abs** Primary abs used were rabbit polyclonal KCa3.1 (MW; 46kDa) 1:50-100 for immunohistochemistry and 1:500-1000 for Western blotting, rabbit polyclonal KCa1.1 α-subunit (MW; 110kDa) 1:100 for immunohistochemistry and 1:500 for Western blotting (Affinity BioReagents), goat polyclonal KCa2.1 (MW; 70kDa) 1:200 (Santa Cruz), rabbit polyclonal KCa2.2 (MW; 70kDa) 1:500 (Lifespan Biosciences), rabbit polyclonal KCa2.3 (MW; 70kDa) 1:500 (Santa Cruz), mouse monoclonal β-actin (MW; 43kDa) 1:1000 (Santa Cruz), goat polyclonal l-caldesmon (MW; ~70kDa) 1:500 (Santa Cruz), mouse monoclonal α-SMA 1:100 (Sigma), rat monoclonal Mac3 1:100 (BD Biosciences), rabbit polyclonal CD3 1:100 (DakoCytomation) and goat polyclonal vWF 1:50-200 (Santa Cruz). Secondary abs were a HRP-labeled donkey anti-rabbit 1:5,000-

10,000, anti-goat ab 1:10,000-20,000, or goat anti-mouse 1:5,000 (Santa Cruz) for Western blotting, and FITC-conjugated donkey anti-rabbit 1:100, Texas red-conjugated donkey anti-mouse 1:100, Texas red-conjugated donkey anti-goat 1:100, Texas red-conjugated chicken anti-rat 1:100 (Santa Cruz) and biotinylated abs included in Vectastain Elite ABC kits or M.O.M. Immunodetection kit (Vector Laboratories).

**EC denudation** Mouse aortas were dissected free of adventitial fat and connective tissue, and cut open longitudinally. ECs were removed without detachment of plaques by gently rubbing the intimal surface with a moist cotton swab under a microscope followed by rinsing as previously reported (5). Supplemental Figure 3 shows EC-intact and –denuded aortic segments in the upper panel and immunostaining for vWF in sections from these aortic segments in the lower panel. EC denudation by this gentle method does not cause the detachment of atherosclerotic plaques, which are seen as irregular white area, in the aortas (right aortic segment) as compared to the EC-intact segment (left aortic segment). The single layer of ECs (arrowhead in Supplemental Figure 3) on the surface of EC-intact aorta (left) is positively stained for vWF in dark brown, while the staining is not observed in EC-denuded aorta (right).

ECs in HCAs and mouse arteries were also mechanically denuded using a modification of a method used previously by us (4;6;7). One end of arteries was cannulated with a glass pipette in a vessel chamber filled with cold HEPES buffer. Following washing in ethanol and rinsing in PBS a human hair was repeatedly inserted through the vessel lumen. Next approximately 2 ml of air were gently passed through the

vessel over a 2-min period. This was immediately followed by HEPES buffer to fill the vessel and remove all air bubbles (4;6;7). Successful removal of ECs by these methods has been confirmed by no immunostaining for vWF. Supplemental Figure 3 shows that ECs (arrowhead) are stained for vWF in an intact HCA (left), but not in a denuded artery (right). We routinely confirm the successful denudation of arteries by demonstrating an impaired vasodilation to an EC-dependent vasodilator (ADP or acetylcholine) and preserved vasodilation to EC-independent vasodilator (papaverine) (4;6;7). In this study, EC denudation abolished vasodilations to 10 μM ADP in HCAs (% maximal dilation; 0 % vs 72±2%) and to 10 μM acetylcholine in mouse carotid artery segments (-18±8 % vs 89±3%), while vasodilations to 100 μM papaverine were not impaired in HCAs (95±3 % vs 90±3%) and in mouse arteries (82±4 % vs 88±4%).

**Mouse aortic SMCs.** Thoracic aortas were dissected from three $KCa3.1^{+/+}$ and four $KCa3.1^{-/-}$ mice and the adventitial tissue trimmed away. The aortas were longitudinally opened and ECs were removed by a cotton swab followed by incubation in the dissecting solution containing 0.5mg/ml collagenase Type 2 (Worthington) and 125 μg/ml elastase (Sigma) DPBS for 10 min at 37 °C. Remaining adventitial tissue and ECs was removed, and the aorta was cut into small pieces and incubated in the solution for 1-2 h at 37 °C. Cell clumps were dissociated by aspiration through a 1.0-ml pipette. The cell suspension was centrifuged at 150×g for 5 min at room temperature and resuspended in SmGM2 (Camblex, Inc.). The isolated cells were characterized as SMCs based on positive immunohistochemistry staining for α-SMA and by morphological characteristics similar

to that observed with human coronary SMCs. Cells between passage 5 and 8 were stocked to match passages of cells from KCa3.1$^{+/+}$ and KCa3.1$^{-/-}$ mice for experiments. After achieving the quiescent state of cells by 48-h incubation in serum-free medium (SmBM), cells were stimulated with 20 ng/ml PDGF in each assay.

**Real-time PCR.** Primer sequences (Integrated DNA Technologies, Inc., Coralville, IA) were as follows: for hKCa1.1 (hslo-alpha), 5'- ACG ACT CTA CTG GGA TGT TTC AC -3' (sense) and 5'- TCG CCA AAG ATG CAG ACC AC -3' (antisense); for hKCa3.1, 5'- GGC CAA GCT TTA CAT GAA CAC G -3' (sense) and 5'- GTC TGA AAG GTG CCC AGT GG -3' (antisense); for GAPDH, 5'- CCT GCC AAG TAT GAT GAC -3' (sense) and 5'- GGA GTT GCT GTT GAA GTC -3' (antisense). QuantiTect Primer Assays (Qiagen) were used for hKCa2.1, 2.2 and 2.3 mRNA analyses. The reaction conditions were as follows: 3 minutes at 95º followed by 40 cycles at 95º for 60 seconds, 60º for 60 seconds.

**siRNA Transfection.** siRNA transfection was performed as previously reported (8). Briefly, 24 h before the transfection, human coronary SMCs were seeded into culture plates ($2x10^5$ cells/well in 100-mm culture dishes, $32x10^4$ cells/well in 6-well plates, or $1x10^4$/well in 96-well plates) with SmBM culture medium (Camblex, Inc.), so that cells were 70-80% confluent at the time of the transfection. KCa3.1-specific siRNA and the negative control (Ambion: Austin, TX) were diluted with Plus Reagent (2µl/ml, Invitrogen, Carlsbad, CA) and then incubated with Lipofectamine Reagents (4µl/ml, Invitrogen) in DMEM (Invitrogen). Cells were transfected in DMEM with the transfection mixture for 3 h. After washout of the mixture and additional 21-h incubation

in SmBM, cells were stimulated with PDGF. Optimization of siRNAs concentration (12.5 nM), transfection time, cell density and other experimental conditions were determined by quantifying KCa3.1 mRNA and protein expression prior to experiments (Supplemental Figure 6).

**Telemetry BP measurement** The pressure-sensing catheter of the TA11PA-C20 BP device (Data Sciences International) was implanted by using the left carotid artery placement as described (9). Briefly mice were anesthetized by isoflurane and then deeply anesthetized with sodium pentobarbital (50 mg/kg i.p., Abbott Laboratories). Using aseptic technique, a ventral midline incision was made in the skin over the throat and the left carotid artery was isolated. The tip of the catheter was inserted into the carotid and inserted until its tip was in the thoracic aorta. The catheter was secured in place with 6-0 surgical silk. The transducer/transmitter/battery was tunneled s.c. and placed along the right flank. The incisions were closed with sterile, 4-0, absorbable suture. The mice were maintained on a heated recovery table until they were fully conscious following the surgery. Postoperative cefazolin (30mg/kg) was given to prevent infection. After a 3- to 5-day recovery period from surgery, daily measurements of mean arterial BP and heart rate were obtained for 3 consecutive days in which the mice were maintained under conscious, unrestrained conditions (10).

**Plasma concentrations of KCa3.1 blockers.** Blockers were dissolved in peanut oil for s.c. or in 25%-cremophor EL (BASF)/PBS solution for i.v. administration. Blood samples were collected at various time points after single s.c. or i.v. injection of 10 or 120mg/kg TRAM-34 or 24 h after continuously daily s.c. treatment with TRAM-34 or clotrimazole

for 12 wk. Plasma was separated by centrifugation and stored at –80°C pending analysis. Samples were purified using C18 solid phase extraction (SPE) cartridges. Elution fractions corresponding to TRAM-34 or clotrimazole were dried under a stream of nitrogen and redissolved in acetonitrile/water (1:1). LC/MS analysis was performed with a Hewlett-Packard 1100 series HPLC stack equipped with a Merck KGaA RT 250-4 LiChrosorb RP-18 column interfaced to a Finnigan LCQ Classic MS. The mobile phase consisted of acetonitrile/water with 0.2% formic acid. The flow rate was 1.0 ml $min^{-1}$ and the gradient was ramped from 20/80 to 70/30 in 5 min, then to 80/20 over 11 min. With the column temperature maintained at 30°C, TRAM-34 eluted at 14.4 min and was detected by a variable wavelength detector (VWD) set to 190 nm and the MS in series. Clotrimazole was analyzed using an isocratic mobile phase of water/acetonitrile 20/80 and it eluted at 6.04 min. Using electrospray ionization MS (capillary temp. of 270°C, capillary voltage of 1V, tube lens offset of –15 V, positive ion mode) TRAM-34 and clotrimazole were quantitated by their common daughter ion peak of 277 m/z (2-chlorotrityl fragment) since their respective the molecular ion peak at 344 have very low abundance. Concentrations were calculated with a 5-point calibration curve from 25 nM to 2.5 μM. The related compound TRAM-46 (base peak of 261 m/z, 2-fluorotrityl fragment) was used as an internal standard.

**Toxicity.** To test TRAM-34 for chronic toxicity, 6 male C57BL/6J ($apoE^{+/+}$) mice in each group were treated with TRAM-34 (120mg/kg/day) or vehicle for 28 d, sacrificed, and blood samples and organs (pancreas, mesenteric lymph nodes, kidney, spleen, reproductive tract, heart, lung, thymus, brain, liver, stomach, small intestine and large

intestine) collected. Analyses of the hematology, the chemistry and the necropsy were performed in the Comparative Pathology laboratory of UCD, in Blood Research Institute of Medical College of Wisconsin, in Marshfield Clinic Laboratories (Brookfield, WI), or in the General Medical Laboratories (Madison, WI).

**Binding studies.** TRAM-34 was screened at 10 μM for potential affinity to a panel of 30 receptors and channels by displacement of standard radioligands at MDS Pharma (http:www.mdsps.com). As is customary in the MDS Pharma Hit Profiling Screen inhibition or stimulation of binding by $\geq$ 50% was considered a significant response.

**Electrophysiology.** HEK293 cells expression Kv11.1 (HERG) were a gift from Craig January, University of Wisconsin, Madison. HERG currents were recorded with a 2-step pulse from –80 mV first to 20 mV for 2 sec and then to –50 mV for 2 sec (11) and the reduction of both peak and tail current by the drug was determined. HEK 293 cells expressing L-type channels (Cav1.2b + β2α) were a gift from Franz Hofmann, Institute für Pharmakology and Toxikologie, Munich, Germany). Cav1.2 currents were elicited by 600-ms depolarizing pulses from –80 to 20 mV every 10 sec with a CsCl based pipette solution and an external solution containing 30 mM BaCl2 (12). Blockade of $Ca^{2+}$ currents was determined as reduction of the current minimum.

**Rat Influenza Host Resistance Model.** The effect of TRAM-34 on host resistance was tested at Burleson Research Technologies Inc. (Morrisville, NC) as previously described (3). Briefly, female Sprague Dawley rats (Charles River, Raleigh, NC) were infected intranasally with $2x10^5$ plaque-forming units of rat-adapted influenza virus (RAIV), sacrificed 1, 2, 4, 8 and 21 days later and lung homogenates tested for plaque forming

units on monolayers of Madin Darby Canine Kidney (MDCK) cells. Rats were treated daily with either vehicle, TRAM-34 (20 mg/kg/d i.p.) or the positive control dexamethasone 21-phosphate (2 mg/kg/d) starting from Day –7 until Day 21.

## Supplemental References


1. Si,H., Heyken,W.T., Wolfle,S.E., Tysiac,M., Schubert,R., Grgic,I., Vilianovich,L., Giebing,G., Maier,T., Gross,V. et al 2006. Impaired Endothelium-Derived Hyperpolarizing Factor-Mediated Dilations and Increased Blood Pressure in Mice Deficient of the Intermediate-Conductance $Ca^{2+}$-Activated $K^{+}$ Channel. *Circ Res* **99**:537-544.

2. Ataga,K.I., Smith,W.R., De Castro,L.M., Swerdlow,P., Saunthararajah,Y., Castro,O., Vichinsky,E., Kutlar,A., Orringer,E.P., Rigdon,G.C. et al 2008. Efficacy and safety of the Gardos channel blocker, Senicapoc (ICA-17043), in patients with sickle cell anemia. *Blood* **111**:3991-3997.

3. Burleson,G.R. 1995. Influenza virus host resistance model for the assessment of immunotoxicity, immunostimulation and anti-viral compounds. In *Methods in Immunotoxicology*. G.R.Burleson, and Munson,A.E., editors. Wiley Liss, Inc. New York. 181-202.

4. Miura,H., Wachtel,R.E., Loberiza,F.R., Jr., Saito,T., Miura,M., Nicolosi,A.C., and Gutterman,D.D. 2003. Diabetes mellitus impairs vasodilation to hypoxia in human coronary arterioles: reduced activity of ATP-sensitive potassium channels. *Circ. Res.* **92**:151-158.

5. Kolodgie,F.D., Virmani,R., Rice,H.E., and Mergner,W.J. 1990. Vascular reactivity during the progression of atherosclerotic plaque. A study in Watanabe heritable hyperlipidemic rabbits. *Circ Res* **66**:1112-1126.

6. Miller,F.J., Jr., Dellsperger,K.C., and Gutterman,D.D. 1998. Pharmacologic activation of the human coronary microcirculation in vitro: endothelium-dependent dilation and differential responses to acetylcholine. *Cardiovasc. Res.* **38**:744-750.

7. Larsen,B.T., Gutterman,D.D., Sato,A., Toyama,K., Campbell,W.B., Zeldin,D.C., Manthati,V.L., Falck,J.R., and Miura,H. 2008. Hydrogen Peroxide Inhibits Cytochrome P450 Epoxygenases Interaction Between Two Endothelium-Derived Hyperpolarizing Factors. *Circ Res* **102**:59-67.

8. Elbashir,S.M., Harborth,J., Lendeckel,W., Yalcin,A., Weber,K., and Tuschl,T. 2001. Duplexes of 21-nucleotide RNAs mediate RNA interference in cultured mammalian cells. *Nature* **411**:494-498.

9. Kaidi,S., Brutel,F., Van,D.F., Kramer,K., Remie,R., Dewe,W., Remusat,P., Delaunois,A., and Depelchin,O. 2007. Comparison of two methods (left carotid artery and abdominal aorta) for surgical implantation of radiotelemetry devices in CD-1 mice. *Lab Anim* **41**:388-402.

10. Cholewa,B.C., and Mattson,D.L. 2005. Influence of elevated renin substrate on angiotensin II and arterial blood pressure in conscious mice. *Exp Physiol* **90**:607-612.

11. Zhou,Z., Gong,Q., Ye,B., Fan,Z., Makielski,J.C., Robertson,G.A., and January,C.T. 1998. Properties of HERG channels stably expressed in HEK 293 cells studied at physiological temperature. *Biophys. J* **74**:230-241.

12. Kolski-Andreaco,A., Tomita,H., Shakkottai,V.G., Gutman,G.A., Cahalan,M.D., Gargus,J.J., and Chandy,K.G. 2004. SK3-1C, a dominant-negative suppressor of SKCa and IKCa channels. *J Biol Chem* **279**:6893-6904.

13. Wulff,H., Miller,M.J., Hansel,W., Grissmer,S., Cahalan,M.D., and Chandy,K.G. 2000. Design of a potent and selective inhibitor of the intermediate-conductance $Ca^{2+}$-activated $K^+$ channel, IKCa1: a potential immunosuppressant. *Proc. Natl. Acad. Sci. U. S. A* **97**:8151-8156.

## Supplemental Figure Legends.

**Supplemental Figure 1. Specificity of the KCa3.1 antibody.** ***Top***: To determine the specificity of the KCa3.1 antibody, HEK 293 cells stably expressing hKCa1.1, hKCa3.1, and rKCa2.2 were stained with the KCa3.1 antibody. Immunofluorescence revealed strong positive staining in HEK 293 cells transfected with hKCa3.1 **(a).** After incubation of the antibody with blocking peptide at 0.2 μg/ml **(b)** or 2 μg/ml **(c)** little or no staining was seen on hKCa3.1 expressing cells. No immunoreaction was observed in cells empty HEK293 cells (**d**), or cells expressing rKCa2.2 **(e)** or hKCa1.1 **(f)**. The antibody was used at 1:40. Magnification is 20X. ***Bottom***: Immunoblot analysis with the KCa3.1 antibody (1:500) was conducted on membrane protein preparations obtained from aortas of $apoE^{-/-}$ mice, and revealed a single band corresponding to the size of KCa3.1 (46kDa). The band disappeared when the antibody was pre-incubated with the KCa3.1 peptide utilized for antibody production. Therefore, immunofluorescence and immunoblotting both verify the specificity of the antibody for KCa3.1.

**Supplemental Figure 2. Histology of control $apoE^{+/+}$ mouse aortas.** In the vascular wall of control $apoE^{+/+}$ mouse aortic roots (left), the expression of vWF, a marker of ECs, was observed only in the intimal layer (middle), and α-SMA, a marker of VSMCs, was in medial layers (right).

**Supplemental Figure 3. EC denudation.** ***(A)*** **Upper**; representative images of EC-intact (upper left) and –denuded (upper right) segments from apoE$^{-/-}$ mouse aortas. EC denudation by gently rubbing the luminal surface of the aortic segments with a moist cotton swab does not cause the detachment of atherosclerotic plaques (irregular white area) in the aortic segment (right) compared to control, the EC-intact segment (left). **Lower;** representative images of sections from either EC-intact and –denuded aortic segments of apoE$^{-/-}$ mice shown in upper panels. The luminal surface of an EC-intact aortic segment (left) was positively stained for vWF in dark brown (arrowhead). In contrast, an EC-denuded aortic segment showed no immunostaining for vWF and no histological signs of plaques' detachment and damage, indicating successful removal of ECs (right). Magnification 40x. ***(B)*** Representative samples of EC-intact and –denuded HCAs stained for vWF. In an EC-intact HCA (left), the luminal surface of vascular wall (arrowhead) was stained for vWF in dark brown, whereas the denuded vessel was not (right). Successful denudation of ECs in human and mouse arteries by this method was also confirmed by the abolishment of EC-dependent vasodilator responses as stated in the manuscript. Magnification 100x. Sections were counterstained with hematoxylin.

**Supplemental Figure 4. Binding studies.** We had previously demonstrated that TRAM-34 exhibits greater than 1000-fold selectivity over KCa1.1, KCa2.2, KCa2.3, Kv1.1, Kv1.2, Kv1.3, Kv1.4, Kv1.5, Kv3.1, Kv4.2, Kir2.1 and Nav1.2 (13). Here, we further confirmed the specificity of TRAM-34 for KCa3.1 in a radioligand-displacement-screen on 30 receptors and transporters. Some minor interactions were observed at 10 μM. At

10 μM TRAM-34 showed inhibited [$^3$H] nitrendipine binding to L-type calcium channels by 77%, [$^3$H] astemizole binding to Kv11.1 (HERG) by 64%, and [$^{125}$I] RTI-55 binding to the norepinephrine transporter by 54%. Functional $IC_{50}$ values of TRAM-34 for ion channels with cross-selectivity were then determined by whole-cell patch-clamp in our own laboratory (Cav1.2: 12±2 μM; Kv11.1 (HERG): 20±3 μM). TRAM-34 thus displays a 1000-fold selectivity for KCa3.1 (IC50 20 nM) over Cav1.2, Kv11.1 and all previously tested ion channels (13), making it unlikely that TRAM-34's effects in vivo are caused by inhibition of other channels than KCa3.1.

**Supplemental Figure 5. Human coronary SMC viability.** The effect of blockers and inhibitors on cell viability was determined by trypan blue exclusion. None of them induced cytotoxicity in cells stimulated with PDGF at doses tested.

**Supplemental Figure 6. KCa3.1 gene silencing with siRNA transfection in human coronary SMCs.** ***(A)*** siRNA transfection 24 h prior to PDGF stimulation abolished the increase in KCa3.1 mRNA expression at 6 h after PDGF (0.7±0.1-fold of control, $p<0.05$ vs PDGF alone 1.6±0.1, n=9). ***(B)*** Representative immunocytofluorescent images of KCa3.1 protein expression are shown in the left panels. Stimulation with PDGF for 48 h significantly increased FITC fluorescent intensity (green) of human coronary SMCs (middle) in the presence of negative control siRNA, compared to control cells (upper). Cells transfected with the siRNA specific to KCa3.1 gene showed much lower

fluorescence (lower) than those with negative control siRNA. As summarized in the right panel, KCa3.1 gene silencing inhibited PDGF-induced increase in KCa3.1 protein expression (n=28-98 cells), consistent with the suppression of the mRNA expression. Magnification 400x

**Supplemental Figure 7. Pharmacokinetics of TRAM-34 in mice. (A)** Total TRAM-34 plasma concentrations following i.v. administration at 10 mg/kg in cremophor EL/PBS (n=4). The data are best fitted as triexponential decay in keeping with a three compartment model. **(B)** Same data as in (A) plotted on a logarithmic scale to better visualize the three slopes. **(C)** Total TRAM-34 concentrations following s.c. administration at 10 mg/kg (n=4 per time point) and 120 mg/kg (n=6 per time point). The bioavailability s.c. as determined by comparing the AUC from i.v. and s.c. injection at 10 mg/kg is very low (0.5%).

**Supplemental Figure 8. Effect of TRAM-34 therapy on endothelial KCa3.1 expression in mice.** Western blot analysis of KCa3.1 expression in aortas of C57BL/6J mice treated with vehicle or TRAM-34 for 4 wk. EC denudation abolished KCa3.1 expression, indicating the majority of this ion channel in the ECs. This expression was not altered by 4-wk treatment with TRAM-34. 50 μg whole cell lysates.

**Supplemental Figure 9. Effect of TRAM-34 treatment on influenza host resistance in rats.** The effect of TRAM-34 on host resistance was tested in the rat influenza host resistance model. In rats infected intranasally with influenza virus, the clearance of the virus was delayed by dexamethasone but not by TRAM-34, indicating that TRAM-34 does not affect viral clearance (n=5 per time point).

**Supplemental Table 1. Clinical parameters after 12-wk therapy in apoE$^{-/-}$ mice.**

| | **apoE$^{+/+}$** | **apoE$^{-/-}$ with vehicle** | **apoE$^{-/-}$ with clotrimazole** | **apoE$^{-/-}$ with TRAM-34** |
|---|---|---|---|---|
| **Body wt (g)** | 28.8±0.7 (n=12) | 29.1±0.5 (n=35) | 24.2±0.7 (n=10) # | 27.5±0.4 (n=32) |
| **Heart wt (mg)** | 141±4 (n=10) | 151±4 (n=20) | 146±6 (n=10) | 142±2 (n=19) |
| **Hw/Bw ratio, mg/g** | 5.0±0.1 (n=10) | 5.1±0.1 (n=20) | 6.1±0.3 (n=10) # | 5.0±0.1 (n=19) |
| **Mean BP (mmHg)** | 105±3 (n=3) | 115±6 (n=7) | 109±5 (n=7) | 118±5 (n=7) |
| **Heart rate (bpm)** | 524±3 (n=3) | 546±11 (n=7) | 566±39 (n=7) | 569±20 (n=7) |

# $p<0.05$ vs apoE$^{+/+}$, apoE$^{-/-}$ mice with vehicle, apoE$^{-/-}$ mice with TRAM-34.

**Supplemental Table 2. Hematology and chemistry after 12-wk therapy in apoE$^{-/-}$ mice.**

| | apoE$^{+/+}$ | apoE$^{-/-}$ with vehicle | apoE$^{-/-}$ with clotrimazole | apoE$^{-/-}$ with TRAM-34 |
|---|---|---|---|---|
| ***Hematology*** | *n=12* | *n=12* | *n=8* | *n=17* |
| **WBC**, $10^3/\mu l$ | 4.4±0.8 | 7.2±1.5 | 8.6±1.0 ***(a)*** | 7.6±1.2 |
| **RBC**, $10^6/\mu l$ | 8.0±0.4 | 8.5±0.4 | 7.1±0.2 | 7.3±0.3 |
| **Hemoglobin**, g/dl | 12.1±0.5 | 12.2±0.4 | 10.8±0.3 | 11.6±0.5 |
| **Hematocrit**, % | 36.6±1.7 | 37.3±2.0 | 33.4±1.1 | 33.6±1.5 |
| **MCV**, fl | 45.6±0.2***** | 44.1±0.4***** | 46.8±0.3 ***(b)**** | 46.4±0.5 ***(b)**** |
| **MCH**, pg | 15.2±0.3 | 14.6±0.5 | 15.1±0.2 | 16.1±0.4 |
| **MCHC**, g/dl | 33.3±0.7 | 33.1±1.0 | 32.2±0.2 | 34.6±0.7 |
| **Platelet**, $10^3/\mu l$ | 425±48 | 417±55 | 256±106 | 455±63 |
| ***Chemistry*** | *n=7* | *n=8* | *n=7* | *n=9* |
| **Total bilirubin**, mg/dl | 2.1±0.8 | 2.7±0.6 | 2.5±0.2 | 1.2±0.5 |
| **AST**, U/l | 125±32 | 97±13 | 128±15 | 108±18 |
| **ALT**, U/l | 43±8 | 34±5 | 24±4 | 41±9 |
| **ALP**, U/l | 54±3 | 66±9 | 36±1 ***(b)*** | 52±7 |
| **γ-GT**, U/l | <3 | 30±2 | 26±3 | 20±9 |
| **Cholesterol**, mg/dl | 70±3 | 1377±82 ***(a)*** | 1905±148 ***(a)*** | 1443±97 ***(a)*** |
| **Triglycerides**, mg/dl | 56±8 | 91±18 | 193±28 ***(a)*** | 173±51 |
| **glucose**, mg/dl | 181±8 | 159±22 | 151±20 | 184±14 |
| **Total protein**, g/dl | 4.2±0.1 | 3.6±0.5 | 5.2±0.1 ***(a)(b)*** | 4.4±0.2 |
| **Albumin**, g/dl | 2.5±0.2 | 2.2±0.2 | 2.1±0.1 | 2.1±0.2 |
| **Globulin**, g/dl | 1.7±0.1 | 1.8±0.3 | 3.1±0.1 ***(a)(b)*** | 2.3±0.3 |
| **BUN**, mg/dl | 25±2 | 18±2 | 20±1 | 24±3 |
| **Creatinine**, mg/dl | <0.2 | <0.2 | <0.2 | <0.2 |
| **Phosphorous**, mg/dl | 7.1±0.6 | 7.1±0.2 | 7.1±0.2 | 7.5±0.7 |
| **Calcium**, mg/dl | 8.9±0.3 | 9.1±0.2 | 10.3±0.2 ***(a)(b)*** | 10.0±0.4 |
| **Sodium**, mmol/l | 143±4 | 147±1 | 150±1 | 148±3 |
| **Potassium**, mmol/l | 6.6±0.2 | 5.6±0.5 | 6.3±0.4 | 6.5±0.4 |
| **Chloride**, mmol/dl | 106±4 | 108±1 | 107±1 | 108±2 |
| **Bicarbonate**, mmol/dl | 22±1 | 20±1 | 19±1 | 18±2 |
| **Anion gap**, mmon/l | 22±1 | 25±1 | 30±1 ***(a)*** | 28±2 |

Blood samples were collected under non-fasting condition. MCV; mean corpuscular volume, MCH; mean corpuscular hemoglobin, MCHC; mean corpuscular hemoglobin concentration. AST; aspartate aminotransferase. ALT; alanine aminotransferase. ALP; alkaline phosphatase, U/l. γ-GT; γ-glutamyl transferase. BUN; blood urea nitrogen. (*****) The MCV in apoE$^{-/-}$ mice is lower than in control apoE$^{+/+}$ mice or in apoE$^{-/-}$ mice treated with either clotrimazole or TRAM-34. The statistical difference in the MCV between clotrimazole- and TRAM-34-treated mouse RBCs versus vehicle-treated RBCs is therefore an artifact, since no difference exists between the MCVs of KCa3.1-blocker-treated and control apoE$^{+/+}$ mouse RBCs. ***(a)*** $p<0.05$ vs apoE$^{+/+}$ mice. ***(b)*** $p<0.05$ vs apoE$^{-/-}$ mice with vehicle.

## Supplemental Table 3. Effect of TRAM-34 therapy on clinical parameters and the toxicity in C57BL/6L (apoE$^{+/+}$) mice.

### *Hematology*

| | Vehicle (n=6) | TRAM-34 (n=6) | P value |
|---|---|---|---|
| **WBC, $10^3$/ml** | 3.1±0.3 | 4.0±0.5 | <0.05 |
| Neutrophil, % | 25±2 | 24±1 | <0.05 |
| Lymphocyte, % | 60±5 | 66±2 | <0.05 |
| Monocyte, % | 12±3 | 9±1 | <0.05 |
| Eosinophil, % | 3.5±1.1 | 1.5±0.3 | <0.05 |
| Basophil, % | 0.2±0.2 | 0.3±0.2 | <0.05 |
| **RBC, $10^6$/ml** | 7.2±0.1 | 6.8±0.2 | <0.05 |
| Hemoglobin, g/dl | 11.8±0.3 | 11.1±0.3 | <0.05 |
| Hematocrit, % | 40±1 | 38±1 | <0.05 |
| MCV, fl | 56±1 | 53±3 | <0.05 |
| MCH, pg | 16±0.3 | 23±7 | <0.05 |
| MCHC, g/dl | 29±1 | 27±2 | <0.05 |
| **Platelet, $10^3$/ml** | 770±15 | 755±29 | <0.05 |

### *Chemistry*

| | Vehicle | TRAM-34 | P value |
|---|---|---|---|
| **AST, U/l** | 202±53 | 104±43 | <0.05 |
| **ALT, U/l** | 53±10 | 28±7 | <0.05 |
| **ALP, U/l** | 148±15 | 144±31 | <0.05 |
| **g-GT, U/l** | <1.0 | <1.0 | <0.05 |
| **Albumin, g/dl** | 3.3±0.1 | 3.2±0.1 | <0.05 |
| **BUN, mg/dl** | 33±2 | 28±2 | <0.05 |
| **Glucose, mg/dl** | 185±21 | 220±11 | <0.05 |
| **Cholesterol, mg/dl** | 77±7 | 65±4 | <0.05 |
| **HDL, mg/dl** | 36±6 | 30±3 | <0.05 |
| **LDL, mg/dl** | <1.0 | <1.0 | <0.05 |

MCV; mean corpuscular volume, MCH; mean corpuscular hemoglobin, MCHC; mean corpuscular hemoglobin concentration. AST; aspartate aminotransferase. ALT; alanine aminotransferase. ALP; alkaline phosphatase, U/l. γ-GT;γ-glutamyl transferase. BUN; blood urea nitrogen.

### *Necropsy*

| | Lung, liver, pancreas, mesenteric lymph nodes, kidneys, spleen, reproductive tract, heart, thymus, brain, stomach, small intestine and large intestine |
|---|---|
| **Vehicle (n=6)** | No significant lesions due to toxicity |
| **TRAM-34 (n=6)** | No significant lesions due to toxicity |

# Supplemental Figure 1. Specificity of the KCa3.1 Antibody

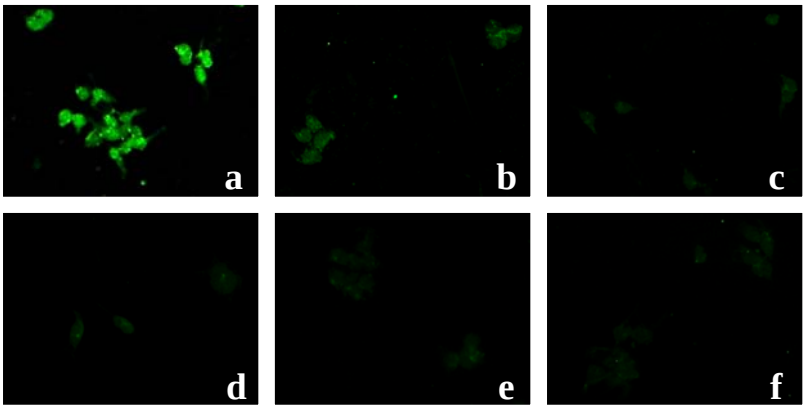


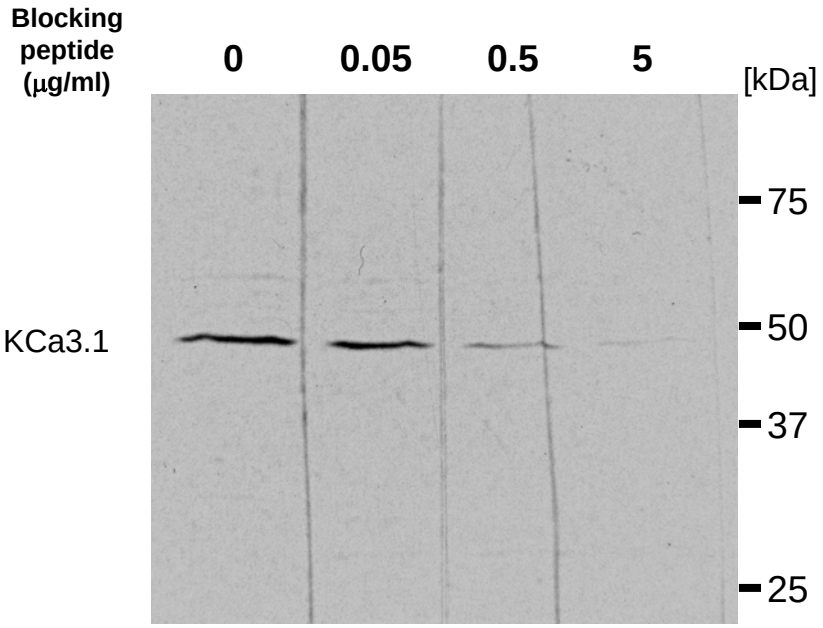


*20 μg membrane protein extracted from aortas of apoE$^{-/-}$ mice*

# Supplemental Figure 2. Control apoE$^{+/+}$ mouse aortas

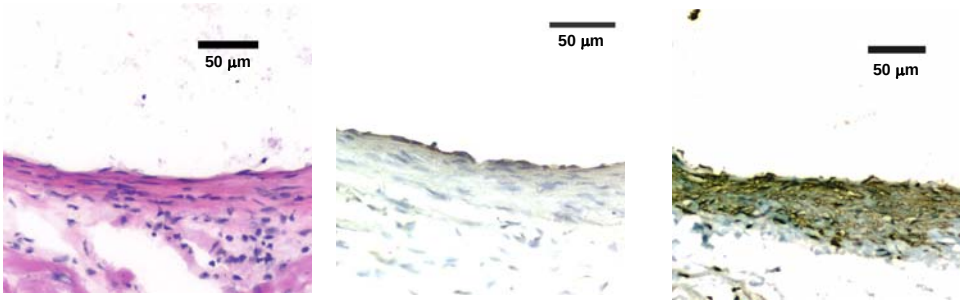


H&E vWF α-SMA

# Supplemental Figure 3. Endothelial denudation

## A. Mouse aortas

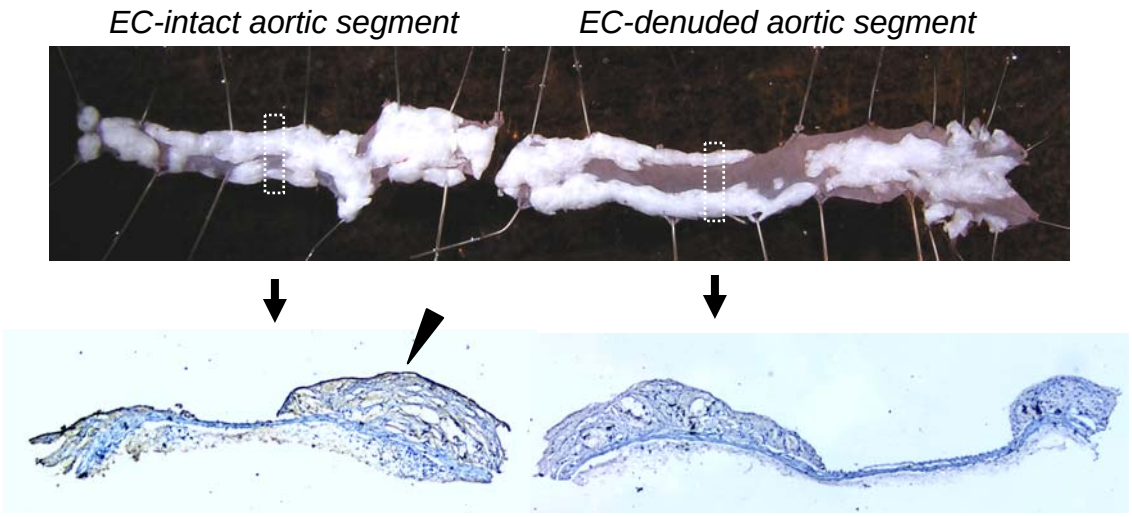


***Immunostaining for vWF***

## B. Human coronary arteries

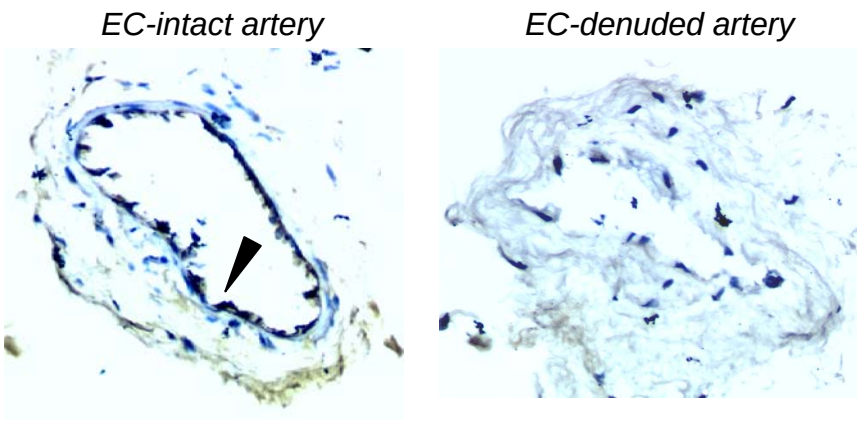


***Immunostaining for vWF***

## Supplemental Figure 4. Receptor and ion channel interaction screening for TRAM-34

| TARGET | SPP. | n= | CONC. | †% INHIBITION % |
|---|---|---|---|---|
| Adenosine $A_1$ | hum | 2 | 10 µM | 18 |
| Adenosine $A_{2A}$ | hum | 2 | 10 µM | 22 |
| Adrenergic $\alpha_{1A}$ | rat | 2 | 10 µM | 6 |
| Adrenergic $\alpha_{1B}$ | rat | 2 | 10 µM | -11 |
| Adrenergic $\alpha_{2A}$ | hum | 2 | 10 µM | 12 |
| Adrenergic $\beta_1$ | hum | 2 | 10 µM | 20 |
| Adrenergic $\beta_2$ | hum | 2 | 10 µM | 17 |
| Calcium Channel L-Type, Dihydropyridine | rat | 2 | 10 µM | 77 |
| Dopamine $D_1$ | hum | 2 | 10 µM | 28 |
| Dopamine $D_{2S}$ | hum | 2 | 10 µM | 7 |
| G Protein-Coupled Receptor GPR103 | hum | 2 | 10 µM | 36 |
| $GABA_A$, Flunitrazepam, Central | rat | 2 | 10 µM | -1 |
| $GABA_A$, Muscimol, Central | rat | 2 | 10 µM | 5 |
| Glutamate, NMDA, Phencyclidine | rat | 2 | 10 µM | 4 |
| Histamine $H_1$ | hum | 2 | 10 µM | 38 |
| Imidazoline $I_2$, Central | rat | 2 | 10 µM | -1 |
| Muscarinic $M_2$ | hum | 2 | 10 µM | -1 |
| Muscarinic $M_3$ | hum | 2 | 10 µM | 3 |
| Nicotinic Acetylcholine | hum | 2 | 10 µM | -11 |
| Nicotinic Acetylcholine α1, Bungarotoxin | hum | 2 | 10 µM | 6 |
| Opiate µ (OP3, MOP) | hum | 2 | 10 µM | 35 |
| Phorbol Ester | mouse | 2 | 10 µM | -12 |
| Potassium Channel [$K_{ATP}$] | ham | 2 | 10 µM | 0 |
| Potassium Channel HERG | hum | 2 | 10 µM | 64 |
| Prostanoid $EP_4$ | hum | 2 | 10 µM | 13 |
| Rolipram | rat | 2 | 10 µM | 4 |
| Sigma $\sigma_1$ | hum | 2 | 10 µM | -10 |
| Sigma $\sigma_2$ | rat | 2 | 10 µM | 8 |
| Sodium Channel, Site 2 | rat | 2 | 10 µM | 23 |
| Transporter, Norepinephrine (NET) | hum | 2 | 10 µM | 54 |

# Supplemental Figure 5. Human coronary SMC viability (Trypan blue assay)

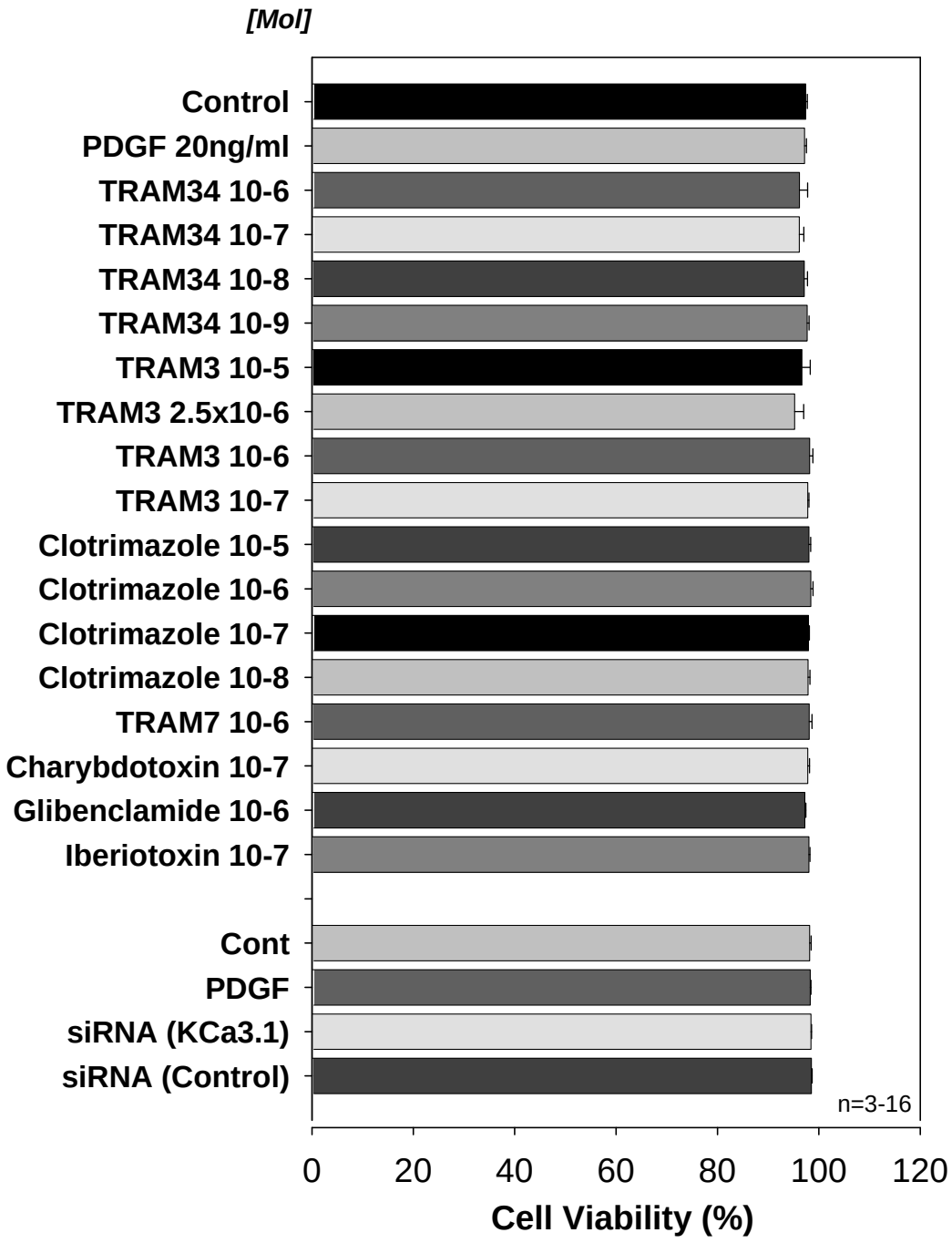

# Supplemental Figure 6. KCa3.1 gene silencing with siRNA

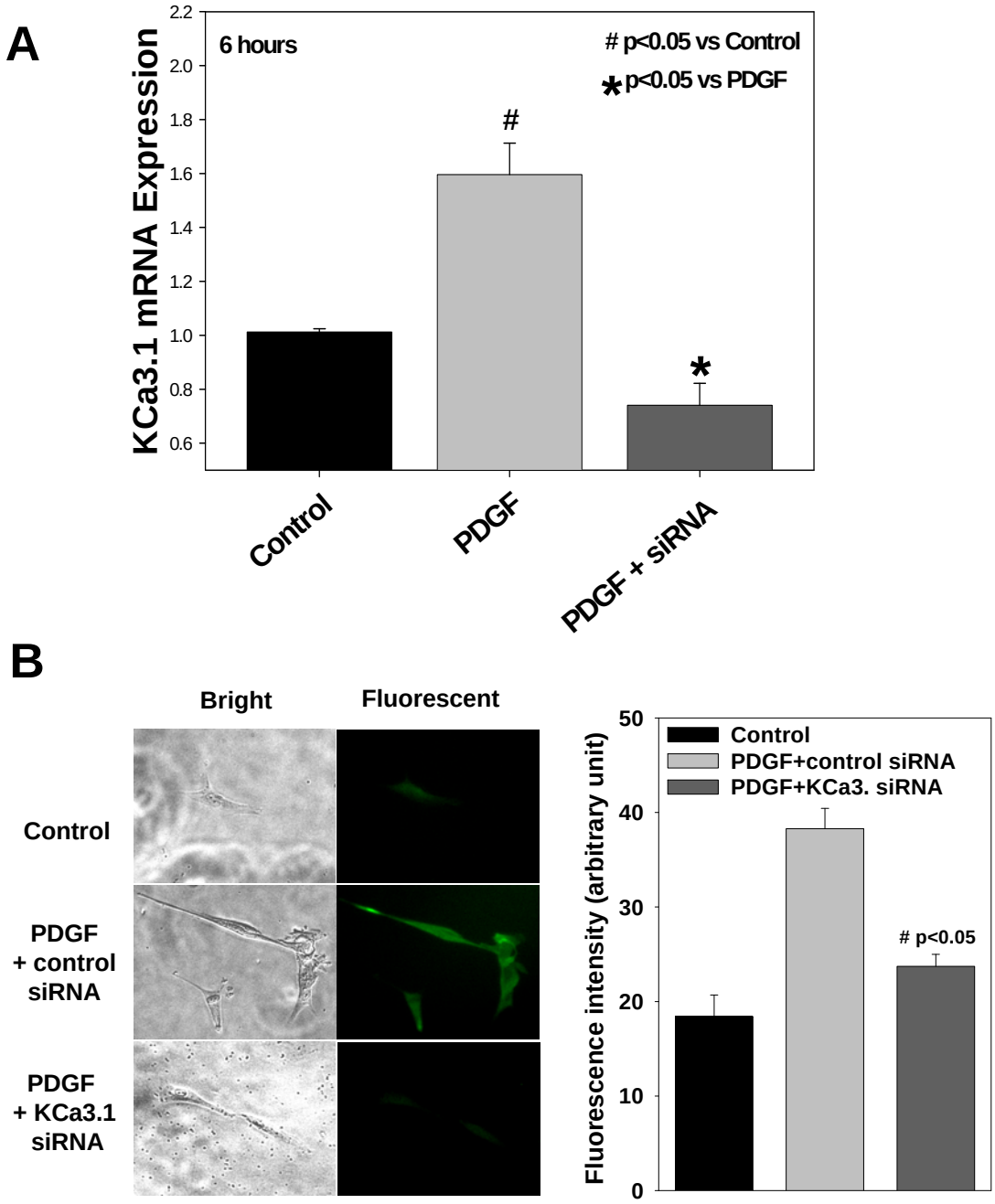

# Supplemental Figure 7. Pharmacokinetics of TRAM-34 in mice

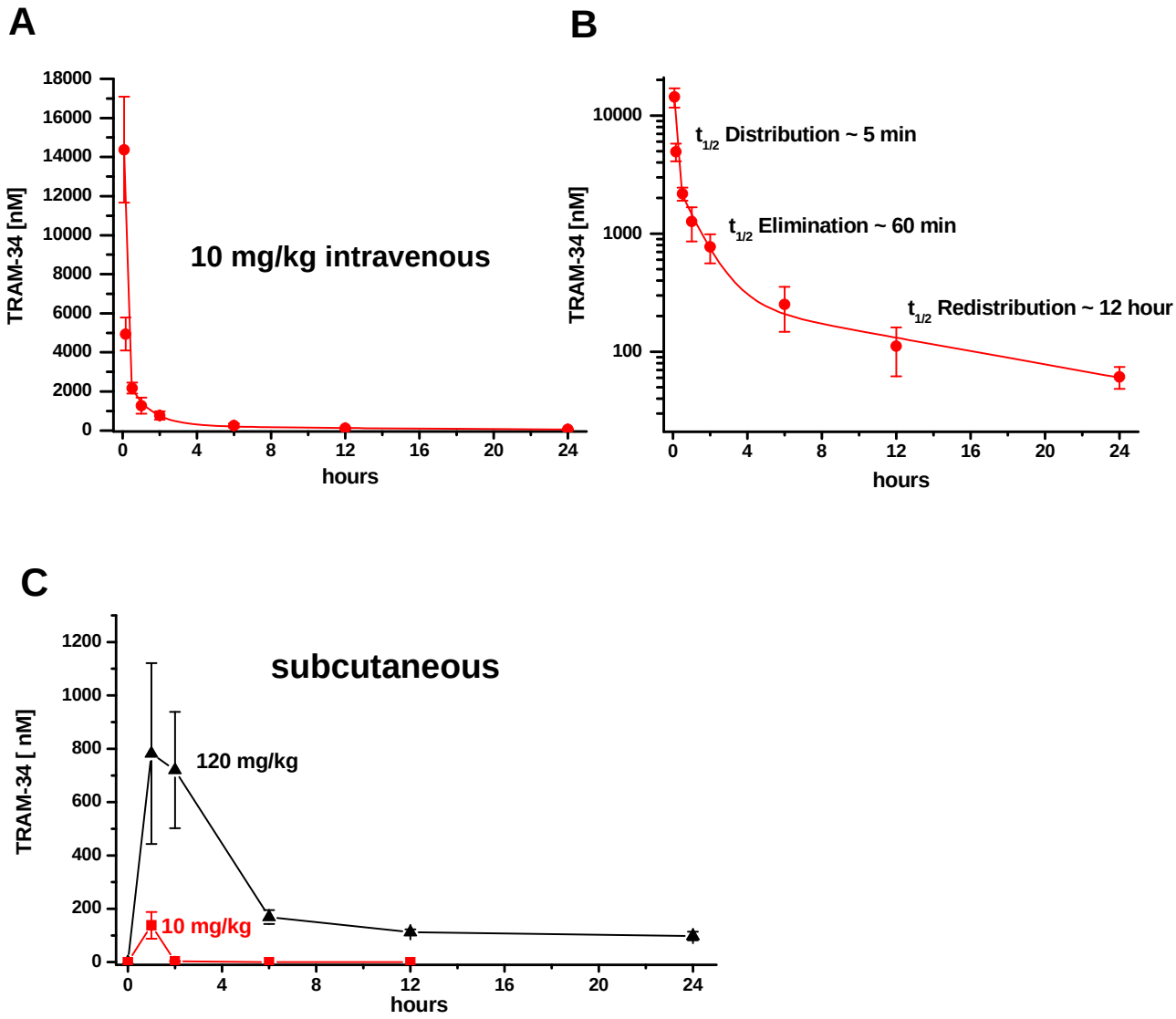

**Supplemental Figure 8. Effect of TRAM-34 therapy on endothelial KCa3.1 expression in C57BL/6L mouse aortas**

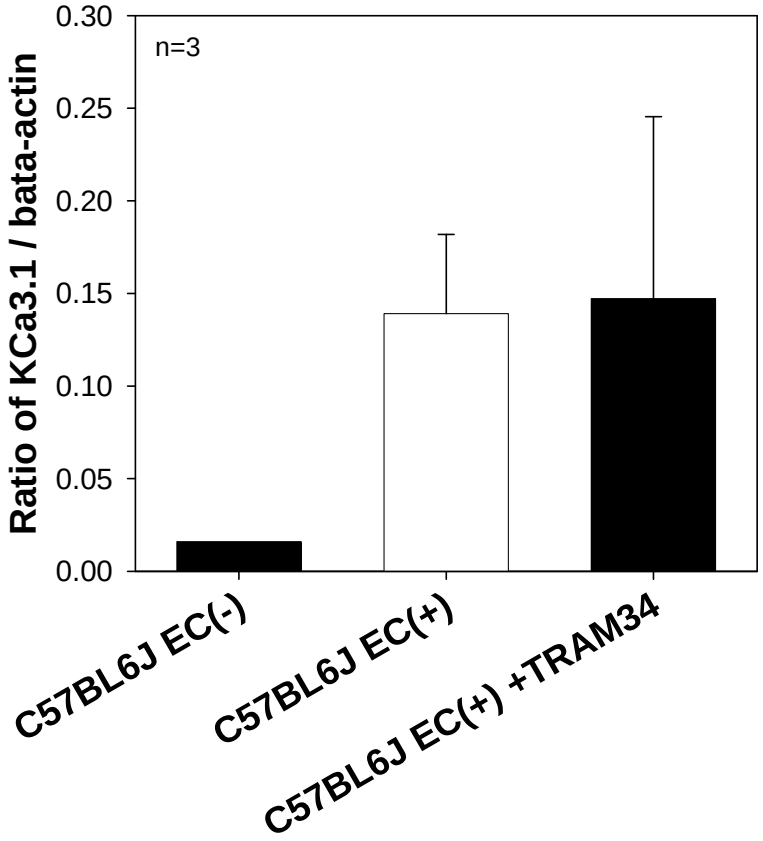

**Supplemental Figure 9. Effect of TRAM-34 treatment on influenza host resistance in rats; clearance of influenza virus**